Journal of Materials and Environmental Science
ISSN : 2028-2508
e-ISSN : 2737-890X
CODEN : JMESCN


J. Mater. Environ. Sci., 2024, Volume 15, Issue 3, Page 397-412

http://www.jmaterenvironsci.com

# Antibacterial and antioxidant activities of Iron Nanoparticles synthesized using *Banana inflorescence* leaf extract

**Sabrin Sultana[1*], Tamana Bhuyan[2], Rajib Saha[3**]**

[1]*Advanced Research Centre, University of Science and Technology, Meghalaya-Ri-Bhoi Meghalaya-793101, INDIA*
[2]*Department of Applied Biology, University of Science and Technology, Meghalaya-Ri-Bhoi Meghalaya-793101, INDIA*
[3]*Department of Physics, University of Science and Technology, Meghalaya-Ri-Bhoi Meghalaya-793101, INDIA*
*Corresponding author, Email address: sultanasabrin19@rediffmail.com*
***Corresponding author, Email address: saharajib26@gmail.com*

***Received*** *28 Feb 2024,*
***Revised*** *12 Mar 2024,*
***Accepted*** *13 Mar 2024*

**Keywords:**
- ✓ Antibacterial,
- ✓ Antioxidant,
- ✓ *Banana inflorescence*,
- ✓ Iron,
- ✓ nanoparticles.

***Citation****: Sultana S., Bhuyan T., Saha R. (2024) Antibacterial and antioxidant activities of Iron Nanoparticles synthesized using Banana inflorescence leaf extract, J. Mater. Environ. Sci., 15(3), 397-412*

**Abstract:** Banana inflorescence is popular and easily available worldwide also it '6. The *Banana inflorescence* leaf can show a great probable for its utilization as a substitute constituent in the medicinal and nutraceutical application. The present manuscript reports the green synthesis of iron oxide nanoparticles from *Banana inflorescence* leaves using ferric chloride hexahydrate as precursor. However, the study aims at assessing the antioxidant properties of green synthesized iron oxide nanoparticles (FeONPs) from *Banana inflorescence* leaf extract along with antibacterial activity against gram negative bacteria *Escherichia coli* (E. coli). X-ray diffraction (XRD), Transmission22 Electron Microscopy (TEM), Field Emission Scanning Electron Microscopy (FESEM), Fourier transform infrared (FTIR), Thermogravimetric analysis/ Differential scanning calorimetry (TGA/DSC) and Zeta potential analysis methods were used to examine the properties of the plant extract Fe nanoparticles. TEM studies identified that the plant extract Fe nanoparticles have the same tetragonal structure as pure mixed-phase. The average size of iron oxide nanoparticles was found to be 40 nm. TGA/DSC results revealed that the temperature beyond 500 ˚C can be considered as the calcination temperature of the synthesized nanoparticles The FTIR analysis predicted the presence of functional groups and the strength of chemical bonds of iron oxide particles in the synthesized plant extract FeONPs. The antioxidant activity was performed by setup test of the 1,1-diphenyl-2-picrylhydrazyl (DPPH) scavenging assay. The antibacterial activity was also determined using Agar Diffusion Method by measuring the Minimum Inhibitory Concentration (MIC) assay. The study reveals that Fe nanoparticles synthesized from *Banana inflorescence* leaf extract showed a good potential for antioxidant and antibacterial activity.

## Abbreviations

| | | | |
|---|---|---|---|
| FeONPs | Iron oxide nanoparticles | PL | Photoluminescence |
| DPPH | 1, 1-Diphenyl-2-picryl-hydrazil | ZP | Zeta potential |
| XRD | X-ray diffraction | *E. coli* | *Escherichia coli* |
| TEM | Transmission electron microscope | MTCC | Microbial Type Culture Collection & Gene Bank |
| FESEM | Field emission scanning electron microscope | DMSO | Dimethyl sulfoxide |
| FTIR | Fourier transform infrared | ZnO-NPs | Zinc oxide nanoparticles |
| TGA | Thermogravimetric analyzer | AgNPs | Silver nanoparticles |

## 1. Introduction

Green approach for the synthesis of metal oxide Nanoparticles (NPs) has received foremost consideration in recent era. Nanotechnology has become promising and widely booming branch of science that has established key success in the age of modern technology. The synthesis of nanoparticles is reliant upon a redox reaction that arises due to the reductive volume of extracellular or cellular components of the cell (Shabbir *et al*. (2023), Tabaght *et al.,* (2022). The synthesis of metal nanoparticles from plant extracts is considered an easy process comparative to fungal/bacteria cultures since fungal and bacterial cultures require decontaminated surroundings and aids to preserve (Buarki *et al*. (2022). There are many advantages in green synthesis, such as being simple, having fast manufacturing procedures, having lower production costs, and producing less waste (Patra *et al*. (2014), (Kiwumulo *et al*. (2022). The use of eco-friendly methods, in the synthesis of metal-based nanoparticle involving plant extracts, has recognized to be a suitable route over the years, due to affluence of preparation, eco-friendliness, and the biocompatible nature of the prepared material with most genetic systems (Adeyemi *et al*. (2022).

However, the plant extracts have the capability to produce NPs with defined size, shape, and composition and due the existence of a varied range of phytochemicals in their extract, it may function as natural stabilizing and/or reducing agents (Hano *et al*. (2022). The synthesis of plant-based NP green is nowadays viewed as a gold standard among other green conventional techniques due to its affluence of use and the multiplicity of plants. (Asif *et al*. (2022) reported a quick, cost free and suitable synthesis of silver nanoparticles using the aqueous leaf extract of *Moringa oleifera* and revealed that biosynthesized Ag NPs can be proved to be an ideal potential candidate for the medical application where antimicrobial activity is essential. Synthesis of gold and silver nanoparticles has been demonstrated by Lomelí-Rosales and his team and found that the plant extract nanoparticles are highly stable and showed suitable antioxidant and antimicrobial activities (Lomelí-Rosales *et al*. (2022). There was study to synthesize and characterize silver nanoparticles from fully expanded leaves of Eugenia roxburghii DC and revealed that the AgNPs effectively inhibit biofilm formation and the biofilm-producing bacterial colonies (Giri *et al*. (2022), Bouammali *et al. (2024)*). The leaf extracts of two medicinal plants viz. *Elaeagnus angustifolia (EA)* were used to synthesized ZnO nanoparticles (NPs) and demonstrated that the plant extract ZnO NPs showed strong antioxidant and antimicrobial activity, could be used as a promising candidate for clinical development (Iqbal *et al*. (2021)). Many researchers have synthesized several NPs from plant extract such as Cu, Au, and Fe etc. and found that this plant extract nanoparticles can show potential application in agriculture, biomedical, and other fields (Alshammari *et al*. (2023), (Botteon *et al*. (2021), (Lakshminarayanan *et al*. (2021).

Magnetic nanoparticles have recently increased great research interest in environmental applications since they possess unique magnetic and electric properties. Presently, the researchers are focusing on the metal nanoparticles owing to the large surface area, low melting point, and good optical, catalytic, electrical and thermal properties (Sivakami *et al*. (2020), Errich et al, (2021)). The main benefit of using plant extracts for synthesis of metal nanoparticles is that they are the insignificant, renewable and non-toxic reducing and stabilizing agents, removing the requirement for expensive polymeric capping agents and stabilizers (Naeimipour *et al*. (2022). (Aida *et al*. (2023) revealed that several herbs, spices and plants containing antioxidants are verified for iron oxide nanoparticle synthesis, as they are responsible for metal ion reduction, aggregation prevention, act as a capping and reducing agent, and stable nanoscale formation. The antimicrobial properties of metallic nanoparticles can be improved by

increasing the solubility of nanoparticles in aqueous media and also by modulating their surface to improve their functionality as antimicrobial compounds (Skłodowski *et al*. (2023), El Hammari *et al,* (2021)). However, metal and metal oxide nanoparticles particle size synthesized from plant extract is the key parameter for determining the antimicrobial efficiency.

*Banana inflorescence* is considered as an ironic source of insoluble fibers and produces medically dynamic compounds such as polyphenols, polysterols, potassium etc. (Pongsuwan *et al*. (2022), Diass et al, (2023)). The interaction of the *banana inflorescence* has yet to be broadly discovered but it is recognized for its immediate configuration and profiles of other nutritious innards, such as fatty acids, amino acids, minerals, etc. that need to be characteristically being examined in detail (Lau *et al*. (2020), Meziane *et al*., (2024)). The green synthesis of nanoparticles is nowadays considered as a total active and environmental treatment technique, is gaining much research attention. It comprises endless consent to produce plant extract-based nanoparticles is a non-toxic and safe process. Moreover, the plants and leaves extracts are used as reducing agents, also no chemical component or pattern are essential in this process which makes this process environment friendly and can be readily use for medical applications. Scanty literatures are available about the study of the leaves of *Banana inflorescence* natural sources for green synthesis of nanoparticles, apart from those on extracts from various parts of the plant. This is significant because the leaves of *Banana inflorescence* become a surplus when after the inner part is used a food item. The phytochemicals from *Banana inflorescence* are believed to serve as a non-toxic source of reducing and stabilizing agents. So, we have investigated the possible use of *Banana inflorescence* leave waste as a leaf extract for synthesis of green nanoparticles. The present study therefore investigates the synthesis of iron nanoparticles using *Banana inflorescence* leaf extract and the effect of its antibacterial and antioxidant properties. The green synthesized iron nanoparticles (FeONPs) were investigated for antibacterial activity against morbific fungus *Escherichia coli* and also its antioxidant activity using DPPH test. The chemical, functional, and morphological properties of the synthesized nanoparticles were characterized using different standard techniques.

## 2. Materials and Methods

### 2.1 Materials and chemicals used

*Banana inflorescence* leaf extract was bought from a local market in Assam, India. Analytical grade ferric chloride hexahydrate ($FeCl_3.6H_2O$), sodium hydroxide pellets (NaOH) were purchased from Merck, India. All chemicals are used without further purification. solvent used in the study were of highest purity and analytical grade purchased from Sigma Aldrich.

### 2.2 Laboratory Preparation of Extracts from Plants

*Banana inflorescence* leaf extract fresh leaves were cleaned by washing under tap water and then rinsed with deionized water. to eliminate contaminants and then dried in the shade at the laboratory temperature of 60 °C for four days. The *Banana inflorescence* along with its leaves are shown in **figure 1 (a) and (b)**.

### 2.3 Preparation of Green Fe Nanoparticles

$FeCl_3.6H_2O$ was used as the precursor for the synthesis of the FeONPs. Biosynthesis of FeNPs was performed using a simple multistep method according to the protocol stated by (Bhuiyan *et al*. (2020) with further modification. 30 mL of the *Banana inflorescence* leaf extract was added dropwise with 30

mL of 0.1M $FeCl_3.6H_2O$ solution in 1:1 ratio at room temperature. The solution mixture was stirred using a magnetic stirrer for 40 min. 1 M NaOH was added to the solution. The resulting solution was again put on a magnetic stirrer for stirring it for 20 min. The formation of strong black colored solution confirmed the synthesis of iron oxide nanoparticles. The FeONPs was cleaned by successive washing with ethanol and water. The NPs were finally dried in a hot air oven at 85 °C for 3 hours and under refrigeration until their characterization and evaluation of antioxidant and antimicrobial activity later. The whole synthesis can be considered as "batch" or "one-pot" synthesis i.e. it is actually performed in one beaker, glass, pot or reactor. **Figure 2 (a) and (b)** represents the *Banana inflorescence* leaf extract and synthesized FeONPs, respectively.

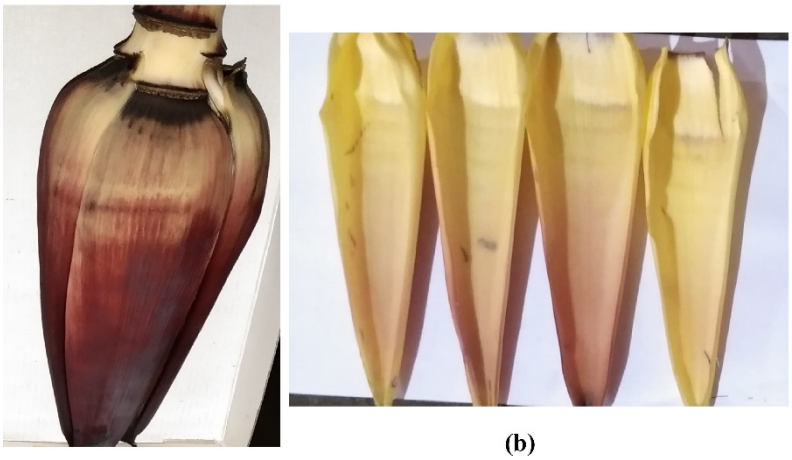

(a) (b)

**Figure 1.** (a) *Banana inflorescence* (b) leaves

**(a)** **(b)**

**Figure 2.** (a) *Banana inflorescence* leaf extract (b) synthesized FeONPs

### 2.4 Instrumentation

UV-Visible Spectrophotometer model (UV 1900 SHIMADZU, Kyoto, Japan) was used to obtain the absorbance spectra of the FeONPs. X-ray diffraction (XRD) spectroscopy model Smartlab (Rigaku Technologies, Japan) was used to measure and compare the structure-property relationship of the

FeONPs. Transmission electron microscope (TEM) electronic spectroscopic was carried out using a JEM-2100 (JEOL, Japan) to determine the particle size, shape and distribution. Single area electron diffraction (SAED) using JEM-2100 (JEOL, Japan) was carried out for obtaining two-dimensional (2D) electron diffraction patterns. FESEM (GEMINI 300, USA) electronic spectroscopic was used to capture the microstructure image of the FeONPs. Fourier transform infrared spectroscopy (FTIR) was carried out using IMPACT 410 (NICOLET, USA) spectrometer to provide details about the chemical bonds that are present in the synthesized NPs. Thermo Gravimetric Analyzer (TGA) (TGA-50 & DSC-60, SHIMADZU, Japan) was used to study the heat loss of the nanoparticles. Photoluminescence (PL) spectroscopy was recorded using LS55 (PERKIN ELMER, USA) to examine the separation of photogenerated charge carriers and Dynamic light scattering (DS) Litesizer™ 500 (ANTON PAAR, Austria) was used for the characterization of the Zeta potential of the synthesized FeONPs. OriginLab Pro 2021 software was used for plotting and peak analysis of the data.

### 2.5 Antibacterial activity

The antibacterial efficacies of biosynthesized iron oxide nanoparticles (FeONPs)were investigated against Gram-negative *E coli*. The bacterial isolates were cultured in nutrient broth and incubated at 37°C with stirring in a magnetic stirrer for 24 h. The colony-forming units (CFU) was constantly retained at ∼106 per mL-1. To prevent clump formation, the inoculated bacterial cultures were incubated under constant shaking conditions at 180 rpm in an incubator shaker.

### 2.6 Agar Diffusion Method

The study investigated the antibacterial activities of the biosynthesized iron oxide nanoparticles (FeONPs) in 24-h bacterial isolates using the Agar-Well diffusion technique (Haile *et al*. (2020), Yahyaoui *et al,* (2014)). The nutrient agar media was sterilized in an autoclave for 30 min at 120 °C. The petri plates were filled with 18 mL of agar media and bacterial cultures (10 µL) were spread out on agar plates aseptically. The agar was allowed to solidify at 37°C, followed by the creation of wells of 5 mm diameter in each plate using a sterile borer. A varying concentration of FeONPs (0, 40, 60, 80 µg mL-1) was introduced in the wells and the plates were incubated for 12 hours at 37 °C. The zone of inhibition surrounded the wells, and the diameter of the clear zone validated the antibacterial effectiveness of the biogenic FeONPs. The experiments were carried out in triplicate, and consistent reliable findings were attained.

### 2.7 Minimum Inhibitory Concentration (MIC) Assay by Microdilution method

The standard microdilution method was performed to investigate the minimum inhibitory activity (MIC) of biosynthesized FeONPs on the growth of inoculated *Escherichia coli* cultures. The bacterial cultures were grown for 24 hours in nutrient broth, and the turbidity of the bacterial suspension was adjusted to 0.5 McFarland to attain a final concentration of 106 CFU mL-1.40 µL of the broth was added to each of the ten sterile 96-multiwell plates. The MIC of the samples was determined by adding 40 µL of FeONPs from the stock solution in the first well. This was followed by preparing two-fold serial dilutions to attain different concentrations of FeONPs in each well (0, 40, 60, and 80 µg mL-1). 50 µL of bacterial colonies were introduced in the wells and the plates were incubated at 37 °C for 24 h. The minimum inhibitory concentration (MIC) of FeO NPs in the well at which no bacterial growth was visible was determined. To confirm the MIC, 0.02% resazurin dye was added, and the color changes was monitored.

### 2.8 Antioxidant activity

The antioxidant activity of the extract was determined by the setup test of the 1,1-diphenyl-2-picrylhydrazyl radical (DPPH), based on process defined by (Villano *et al*. (2007) with some modifications. The DPPH test is a commonly used test in the study of antioxidant activity. Ascorbic Acid ($C_6H_8O_6$) was used as standard in determining the percentage of radical scavenging activity. For this test, 1 ml of 4 different concentrations (30, 50, 80 and 100 µg/ml) of FeONPs was mixed with 1 ml freshly prepared DPPH (1 mM in methanol) solution. The DPPH radical solution was mixed in methanol and the solution was stirred strongly for reaction time of 30 minutes. The absorbance of the mixture was determined at 718 nm using UV-Vis spectrophotometer. In the antioxidant test, the DPPH was used as a positive control, whereas the methanol was used as a blank solution. The decrease of the DPPH radicals by an antioxidant causes deformity of the test solution.

## 3. Results and Discussion

### 3.1 UV-Vis

The UV–Visible absorption spectra of the aqueous extract of *Banana inflorescence* leaves were detected at a wavelength range of IONPs at 200-800 nm. **Figure 3** represents the UV-Visible spectrum of green synthesized FeONPs. As seen in the Fig, maximum absorbance was observed at 225 nm, indicated the formation of FeONPs. There was no absorption detected after 500 nm, indicating the complete reduction and formation of iron oxide nanoparticles (Razack *et al*. (2020). (Lathakumari *et al*. (2022) revealed that the Surface Plasmon Resonance (SPR) of bare FeO nanoparticles was observed in the range between 190 and 250 nm which resembles to that of magnetite. The UV-Vis result is quite parallel to those earlier were reported for green FeONPs nanoparticles (AL-Husseini *et al*. (2021), (Sulthana *et al*. (2022).

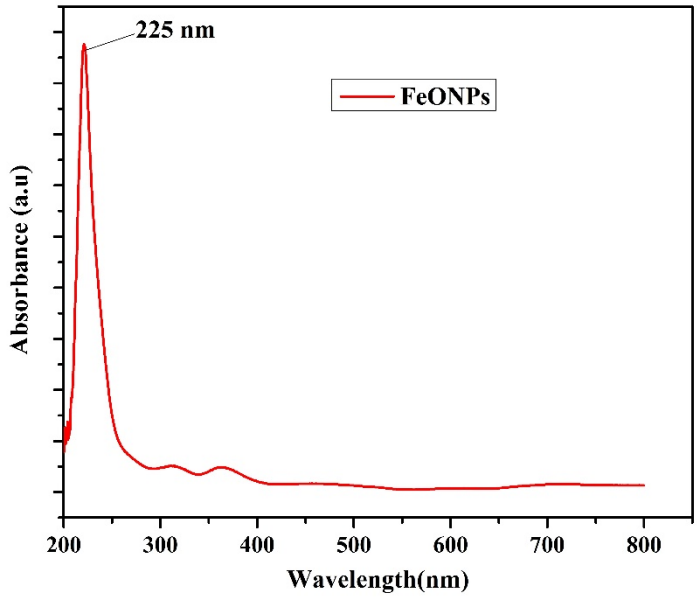


**Figure 3.** UV-Visible Spectra of FeONPs

### 3.2 XRD

**Figure 4** shows the X-ray diffraction spectrum of the synthesized FeONPs using the *Banana inflorescence* leaf extract. XRD analysis generated the peaks for the synthesized FeONPs positioned at 2θ angles of 20.46˚, 23.06˚, 30.01˚, 32.80˚, 47.02˚ and 58.40˚ that corresponds to the crystal planes of (200), (210), (220), (302), (401) and (511), respectively. The intense and sharp peaks shown in the

figure represent indicates that $Fe_2O_3$ nanoparticles formed by the reduction method using *Banana inflorescence* leaf extract were crystalline in nature. The results are nearly comparable to the results obtained for iron oxide nanoparticles using plant extract by other researchers (Buarki *et al*. (2022), (Kiwumulo *et al*. (2022). The XRD peaks of iron oxide nanoparticles calcined at temperature more than 500 °C demonstrate the formation of both magnetite and hematite phase (Mohamed *et al*. (2023). The average crystallite size as determined using the Debye-Scherrer equation was found to be 12.58 nm.

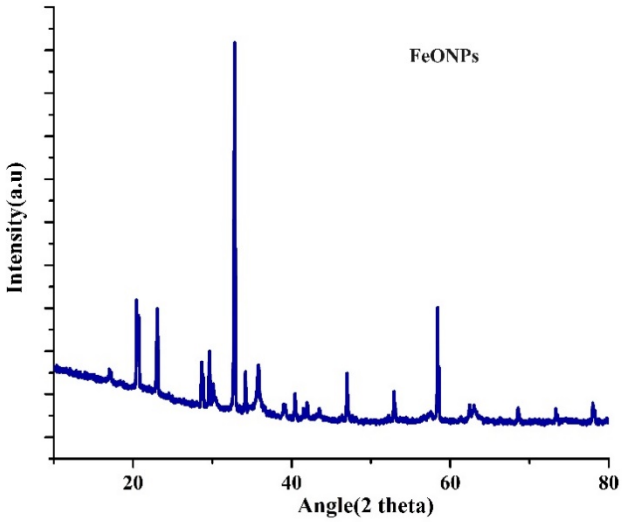


**Figure 4.** X-ray diffraction graph of synthesized FeONPs

### 3.3 TEM

The internal morphology, shape and size of the synthesized FeONPs was studied using TEM and SAED are shown in **figure 5 a & b**. The micrographs confirm the crystalline structure of FeONPs synthesized. An even particle size distribution can be noticed in the synthesized nanoparticles. The SAED pattern revealed that the synthesis process resulted in alike crystalline structures at nanoscale was successfully synthesized. Average particle size was found to be 40 nm which was determined from TEM micrograph.

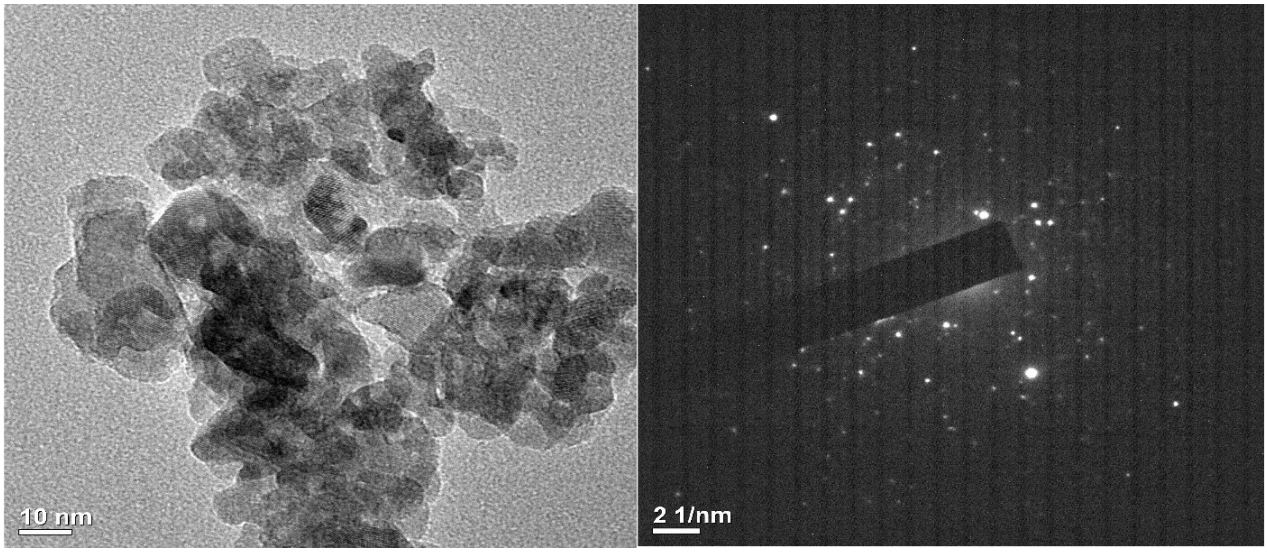


**Figure 5.** TEM micrograph of synthesized FeONPs

### 3.4 FESEM

The FESEM image for the FeONPs is shown in **Figure 6**. The FESEM image displayed that the synthesized nanoparticles are sphere-shaped like and in the range of nanoscales. The average crystalline size of the FeONPs was found to be in the range 80-100 nm. The FESEM analysis showed strong scattering that improved the nanoparticles appearances.

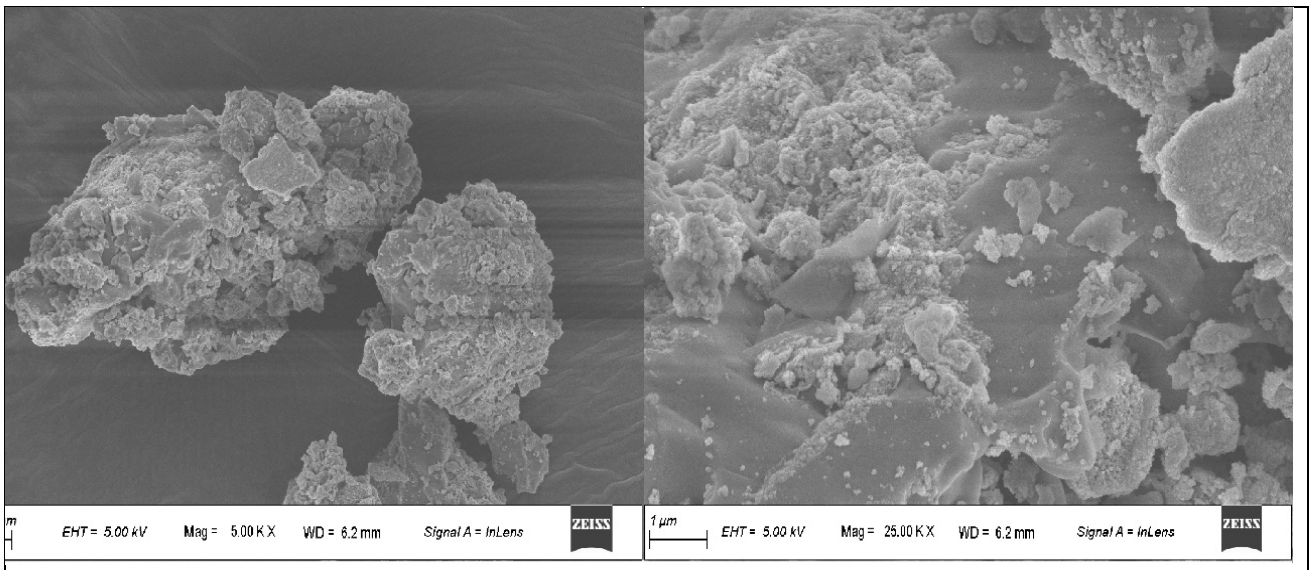


**Figure 6.** FESEM micrographs of synthesized FeONPs

### 3.5 FTIR

The surface chemistry of the synthesized FeONPs was studied using FTIR analyses. **Figure 7** shows the FTIR transmittance graph of the synthesized FeONPs. The FTIR spectra produced from FeONPs synthesized from *Banana inflorescence* leaf extract revealed significant absorption peaks at 3121, 1637, 1391, 1080, and 601 $cm^{-1}$ as shown in the figure. The occurrence of O-H modes of C-OH (3121 $cm^{-1}$) lead the for the stretching and blending vibration band to be broad and prominent are observed in the figure. The peak at 601 $cm^{-1}$ corresponds to the Fe-O stretches. The vibration peaks at the lower wavenumber bands at a range from 400-660 $cm^{-1}$ belongs to the iron oxide nanoparticles (Demirezen *et al*. (2019). However, the additional peak of 1080 $cm^{-1}$ corresponds to C-C stretching, whereas the peak position at 1391 $cm^{-1}$ represents to bending vibration of H-C-H, respectively. Thenmozhi et al., demonstrated that the FTIR characteristic absorption peak at 1637 $cm^{-1}$ represents carbonyl group in the synthesized FeONPs (Thenmozhi *et al*. (2019). Thus, the FTIR results can be recognized that FeONPs are formed and broadly interrelated with the components of the *Banana inflorescence* leaf extract.

### 3.6 PL

**Figure 8** shows the photoluminescence absorption spectra and the calculated band gap of the synthesized FeONPs. PL spectra of the synthesized nanoparticles are independent of the excitation density. A strong change in the spectral shape was detected for the nanoparticles. The maximum emission of the recorded transmission spectra for FeONPs was found to be 565 nm. PL spectra in hematite nanoparticles cover a broad range from UV to near the orange visible region. A research group highlighted that the PL spectra of hematite nanoparticles cover a wide range from UV to near visible

region in the range 363 nm-592 nm due to surface alteration (Archana *et al*. (2021). Moreover, (Ismail *et al*. (2021) reported that PL spectra recorded transmission spectra of FeONPs synthesized using plant extract varies from 480-550 nm.

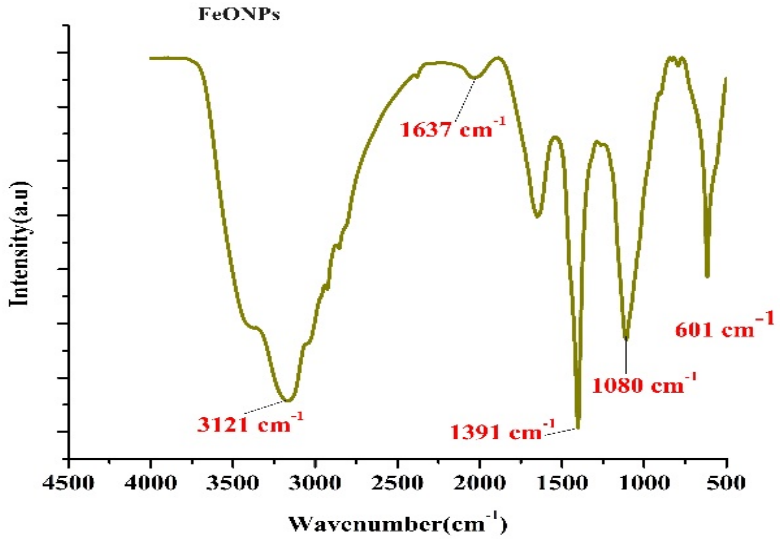


**Figure 7.** FTIR spectra of synthesized FeONPs

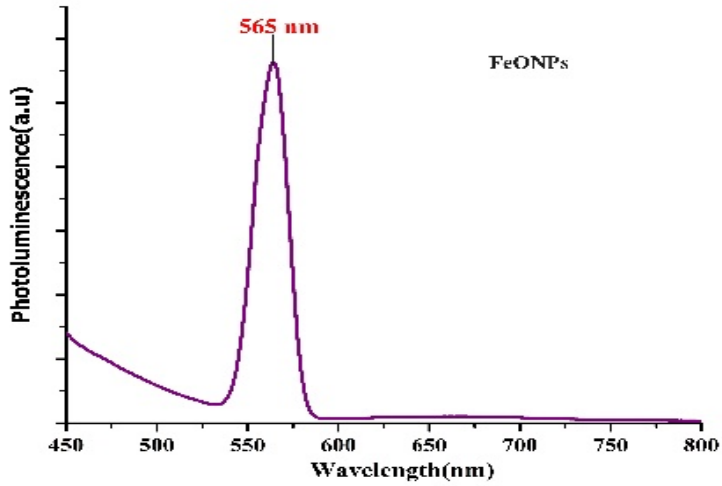


**Figure 8.** PL spectra of synthesized FeONPs

### 3.7 TGA/DSC

The TGA/DSC plot was used to determine the Mass changes of the synthesized FeONPs as a function of increasing temperature. The INOPs was heated at a continuous rate under $N_2$ atmosphere with range of 20 ˚C/10.0 (k min−1)/700 ˚C. The TGA/DSC graph of the FeONPs is shown in **figure 9**. At a temperature of around 220 ˚C, the TGA curve showed a weight loss of around 34.38 % in the study. The obtained weight loss may be ascribed to the exclusion of water molecules removed by nanoparticles from the atmosphere, through which the weight of the synthesized nanoparticles is nearly stable, signifying the nanoparticles thermal stability (Alshammari *et al*. (2023). In DSC analysis, a broad endothermic peak at 270 ◦C indicates the evolving of water molecules, whereas an exothermic peak at 800 ◦C, supports the formation of crystalline particles with phase-chemical purity that is in good agreement with earlier reports (Kannan *et al*. (2023). The slight weight loss (~17.39%) observed

between 400 °C and 530 °C is accredited to evaporation of water, whereas a major peak (34.38%) occurring between 180 °C and 250 °C is being credited to the loss of the organic part of the starting material. In TGA/DSC analysis, the temperature beyond or above which the weight loss is constant is used as the calcination temperature of the synthesized nanoparticles (Herlekar *et al*. (2015) (Geneti *et al*. (2022). Thus, these results could be ascribed to the breakdown of the essence of the leaf extract covered on the synthesized FeONPs.

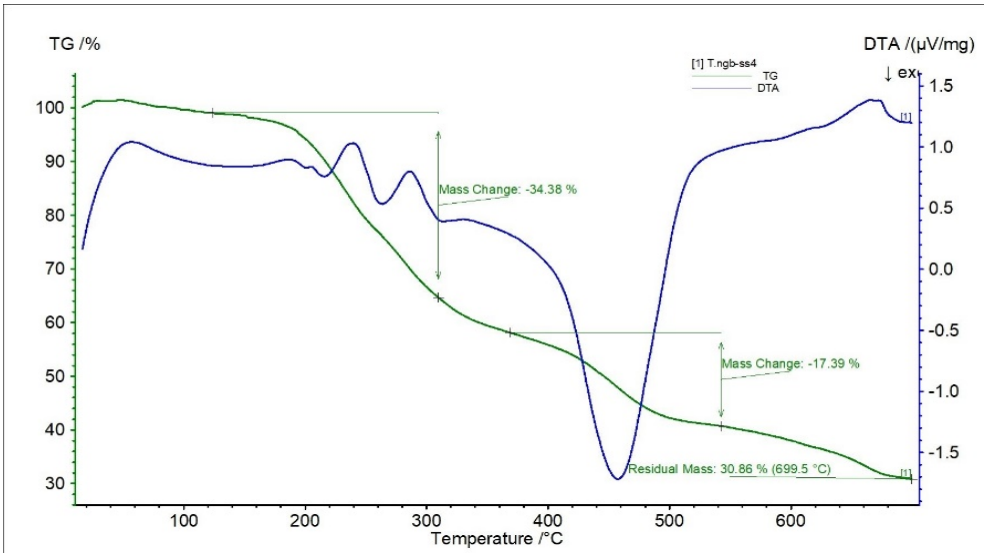


**Figure 9.** TGA/DSC curve of synthesized FeONPs

### 3.8 Zeta potential

The stability of colloidal dispersions of FeONPs is studied using Zeta potential analysis. The Zeta potential of the synthesized FeONPs was found to be -11.9 mV. Zeta potential predicts that for higher the complete Zeta potential value and the smaller the size of the distributed particles, the stability of the particles is greater (Meng *et al*. (2020). Singh and his team reported that the Zeta potential of FeONPs using leaf extract was found to be 19.5 mV that specify soberly stable of the nanoparticles (Singh *et al*. (2020). The mean zeta potential peak of synthesized FeONPs is shown in **figure 10**. The obtained zeta potential value recommended that the colloid of the FeONPs was found to be highly stable that could further improve the stability of the nanoparticles.

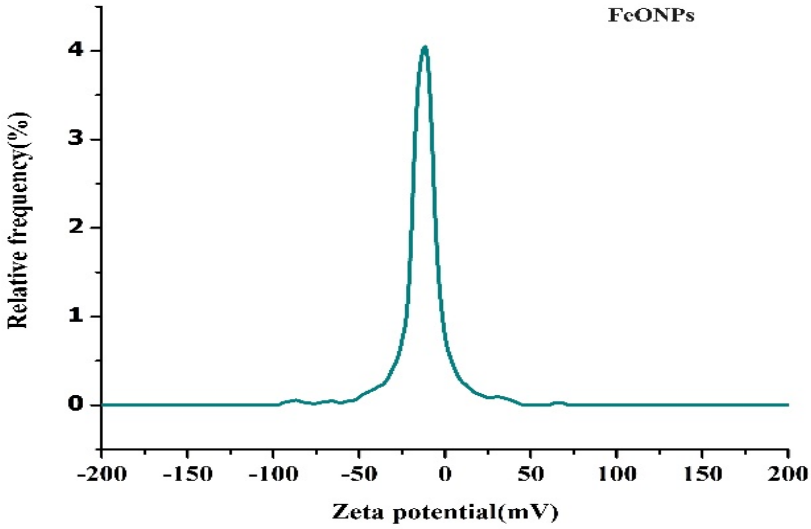


**Figure 10.** Zeta potential graph of synthesized FeONPs

### 3.9 Antibacterial activity

A qualitative agar well diffusion assay was carried out to evaluate the antibacterial activity of as obtained FeONPs on *Escherichia coli*. A varying concentration of FeONPs (0, 40, 60, 80 µg $mL^{-1}$) was added onto the agar wells. The growth inhibition efficacy of FeONPs was confirmed by the presence of clear inhibition zones surrounding the wells on the agar plates, shown in the Figure 9. The MIC of the biosynthesized FeONPs against *Escherichia coli* was found to be 20 µg $mL^{-1}$. It was observed that the diameter of the clear inhibition zones progressively increased with an increase in the concentration of FeONPs. For instance, the zone of inhibition around the control, 20, 40, and 60, and 80µg $mL^{-1}$ was found to be 0, 10.00±0.81 mm, 17.66±0.47 mm and 25.66±0.47 mm respectively, as displayed in **figure 11 (a) - (d)**.

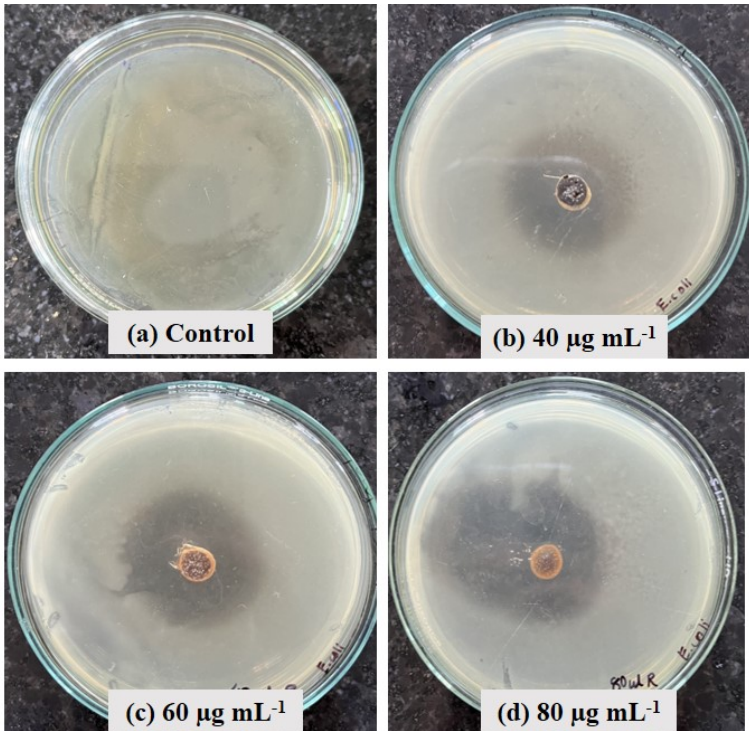


**Figure 11**. Bacteria grown on nutrient agar: (a) control bacteria. Bacteria treated with (b) 40 µg $mL^{-1}$ FeONPs; (c) 60 µg $mL^{-1}$ FeONPs; and (d) 80 µg $mL^{-1}$ FeONPs

The larger zone of inhibition indicated that the bacteria are more sensitive to FeONPs, thus validating the antibacterial activity of the nanostructures. The diameter of the clear inhibition zones (in mm) formed around different concentrations of the samples has been represented in **Table 1**. From the experiments, it can be confirmed that the biosynthesized FeONPs exhibited a significant impact on their ability to inhibit the growth of pathogenic bacterial isolates.

**Table 1.** Average zones of inhibition (in mm) produced by biosynthesized FeONPs on Escherichia coli

| Concentration of $Fe_3O_4$ NPs (µg $mL^{-1}$) in wells | Zone of inhibition (mm) |
|---|---|
| Control | 0 |
| 40 | 8 ± 0.41 |
| 60 | 11 ± 1.33 |
| 80 | 14 ± 1.05 |

### 3.10 Antioxidant activity

DPPH scavenging assays were carried out to regulate the antioxidant activity of *Banana inflorescence* leaf extract FeONPs as shown in **figure 12**. Ascorbic acid was used as a positive control in the similar concentration range. The DPPH was concentrated to the shaped steady, diamagnetic molecule when the nanoparticle was mixed with the solution resulting in altering the color of the solution (Tabassum *et al*. (2023). The DPPH scavenging activity at four different concentrations of the nanoparticles, 30 µg $ml^{-1}$, 50 µg $ml^{-1}$, 80 µg $ml^{-1}$, 100 µg $ml^{-1}$, among which the higher antioxidant activity of 87% was achieved at 100 µg/ml respectively.

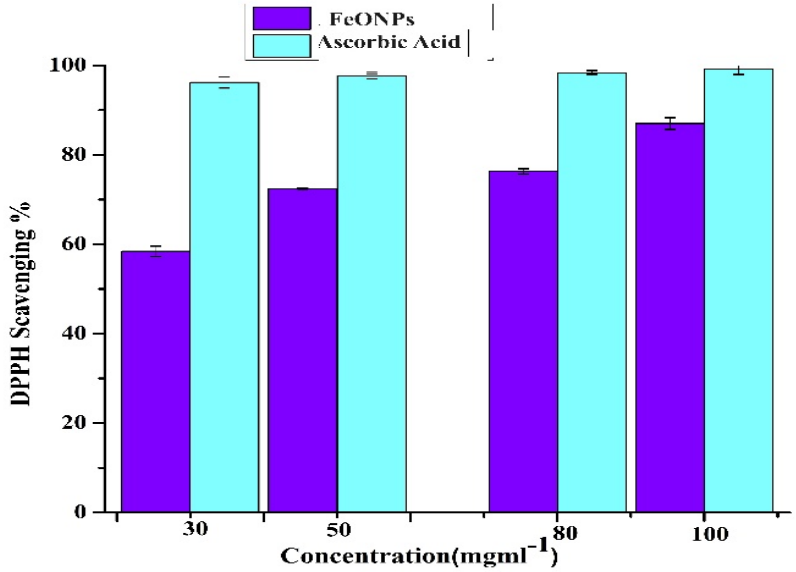


**Figure 12.** Percentage of Antioxidant of synthesized FeONPs and Ascorbic acid

The radical scavenging activities of the synthesized nanoparticles can be attributed to the existence of bioactive components in the extract that hold good antioxidant activity and thus the surface functionalized iron oxide nanoparticles display substantial scavenging activity against free radicals (Yarla *et al*. (2012) (Sandhya *et al*. (2020). The scavenging activity result exhibited that the antioxidant potential of the synthesized FeONPs are free scavengers. The assay was dose-dependent, as seen in the figure. However, in comparison to ascorbic acid at the same concentration, the DPPH scavenging activity of iron oxide nanoparticles was lower in the range from 57% to 87%.

## Conclusion

The aqueous leaf extract of *Banana inflorescence* was used to successfully synthesize FeONPs. XRD, TGA/DSC, and Zeta potential techniques were used to identify the crystallite size, thermal stability, and colloidal stability of the synthesized FeONPs. FESEM images revealed that the crystalline size of the FeONPs was in the range 80-100 nm. FTIR results revealed significant absorption peaks at 3121, 1637, 1391, 1080, and 601 $cm^{-1}$, respectively. TEM micrographs demonstrated that the FeONPs showed an average particle size was found to be 40 nm. Ascorbic acid was used as a positive control in the antioxidant test and FeONPs was used to scavenge free radicals using DPPH. The *Banana inflorescence* leaf extract FeONPs showed higher antioxidant activity of 87% at 100 µg/ml. The synthesized leaf extract FeONPs have showed potential antibacterial activity. The FeONPs synthesized

from the plant leaf extract of *Banana inflorescence* using a simple method that is modest and informal to use without any definite instruments. Thus, the leaf extract FeONPs showed good results antibacterial and antioxidative activity and find its application in various medical assessments.

**Acknowledgement**
The authors acknowledge Department of chemistry, USTM for providing chemicals support to carry out this work. The Central Instrument Facility (CIF), at USTM, Meghalaya and IIT, Guwahati and Sophisticated Analytical Instrumentation Centre (SAIC) at Tezpur University, Tezpur are gratefully acknowledged for assistance in characterization.

**Disclosure statement:** *Conflict of Interest:* The authors declare that there are no conflicts of interest.
*Compliance with Ethical Standards:* This article does not contain any studies involving human or animal subjects.

## References

Adeyemi, J.O., Oriola, A.O., Onwudiwe, D.C., Oyedeji, A.O. (2022). "Plant Extracts Mediated Metal-Based Nanoparticles: Synthesis and Biological Applications". *Biomolecules*. 12(5), 627. https://doi.org/10.3390/biom12050627.

Aida, M.S., Alonizan, N., Zarrad, B. and Hjiri, M. (2023). "Green synthesis of iron oxide nanoparticles using Hibiscus plant extract". *J. Taibah Univ. Sci*., 17(1), 2221827. https://doi.org/10.1080/16583655.2023.2221827.

AL-Husseini, A.H., Sih, B.T. and Al-araji, A.M. (2021). "Green synthesis of iron oxide nanoparticles (Fe2O3) using saffron extract". *J. Phys.: Conf. Ser*., 2114, 012082. https://doi.org/10.1088/1742-6596/2114/1/012082.

Aljabal A.A.A., Akkam, Y., Al Zoubi, M.S., Al-Batayneh, K.M. *et al*. (2018). "Synthesis of Gold Nanoparticles Using Leaf Extract of Ziziphus zizyphus and their Antimicrobial Activity". *Nanomaterials (Basel)*. 8(3), 174. https://doi.org/10.3390/nano8030174.

Alshammari, S.O., Mahmoud, S.Y. and Farrag, E.S. (2023). "Synthesis of Green Copper Nanoparticles Using Medicinal Plant Krameria sp. Root Extract and Its Applications". *Molecules*, 28(12), 4629. https://doi.org/10.3390/molecules28124629.

Archana, V, Prince, J.J. and Kalainathan, S. (2021). "Simple One-Step Leaf Extract-Assisted Preparation of α-Fe2O3 Nanoparticles, Physicochemical Properties, and Its Sunlight-Driven Photocatalytic Activity on Methylene Blue Dye Degradation". *J. Nanomater*., 8570351. https://doi.org/10.1155/2021/8570351.

Asif, M., Yasmin, R., Asif, R., Ambreen, A., Mustafa, M., Umbreen, S. (2022). Green Synthesis of Silver Nanoparticles (AgNPs), Structural Characterization, and their Antibacterial Potential. Dose Response. 20(1), 15593258221088709. doi: 10.1177/15593258221088709.

Bhuiyan, M.S.H., Miah, M.Y., Paul, S.C., Aka, T.D. *et al*. (2020). "Green synthesis of iron oxide nanoparticle using *Carica papaya* leaf extract: application for photocatalytic degradation of remazol yellow RR dye and antibacterial activity". *H*eliyon, 6(8), e04603. https://doi.org/10.1016/j.heliyon.2020.e04603.

Botteon, C.E.A., Silva, L.B., Ccana-Ccapatinta, G.V. et al. (2021) "Biosynthesis and characterization of gold nanoparticles using Brazilian red propolis and evaluation of its antimicrobial and anticancer activities". Sci Rep 11, 1974. https://doi.org/10.1038/s41598-021-81281-w

Bouammali, H., Linda Z., Ziani I., Merzouki, M., Bourassi, Lamiae., Fraj, e., Challioui, A., Azzaoui, K., Sabbahi, R., Hammouti, B., and et al. (2024). "Rosemary as a Potential Source of Natural Antioxidants and Anticancer Agents: A Molecular Docking Study" *Plants* 13. 1: 89. https://doi.org/10.3390/plants13010089

Buarki, F., AbuHassan, H., Al Hannan, F. and Henari, F. Z. (2022). "Green Synthesis of Iron Oxide Nanoparticles Using *Hibiscus rosa sinensis* Flowers and Their Antibacterial Activity". *J Nanotechnol*., 5474645, 1-6. https://doi.org/10.1155/2022/5474645.

Demirezen, D.A., Yıldız, Y.Ş., Yılmaz, S. and Yılmaz, D. (2019) "Green synthesis and characterization of iron oxide nanoparticles using *Ficus carica* (common fig) dried fruit extract". *J. Biosci. Bioeng*., 127(2), 241-245. https://doi.org/10.1016/j.jbiosc.2018.07.024.

Diass, K., Merzouki, M., Elfazazi, K., Azzouzi, H., Challioui, A., Azzaoui, K., Hammouti, B., Touzani, R., Depeint, F., Ayerdi Gotor, A., and et al. (2023). Essential Oil of Lavandula officinalis: Chemical Composition and Antibacterial Activities. *Plants* 12, 7: 1571. https://doi.org/10.3390/plants12071571

El Hammari, L., Latifi, S., Saoiabi, S., Azzaoui, K., Hammouti, B., Chetouani, A., Sabbahi, R.. (2022). Toxic heavy metals removal from river water using a porous phospho-calcic hydroxyapatite. *Mor. J. Chem*. 10 (1), 062 – 072. https://doi.org/10.48317/IMIST.PRSM/morjchem-v10i1.31752

Errich, A., Azzaoui, K., Mejdoubi, E., Hammouti, B., Abidi, N., Akartasse, N., Benidire, L., EL Hajjaji, S., Sabbahi, R., Lamhamdi, A. (2021). Toxic heavy metals removal using a hydroxyapatite and hydroxyethyl cellulose modified with a new gum Arabic. *Indonesian Journal of Science and Technology*. 6, (1), 41 – 64. https://doi.org/10.17509/ijost.v6i1.31480

Geneti S.T., Mekonnen, G.A., Murthy, H.C.A., Mohammed, E.T. *et al*. (2022). "Biogenic Synthesis of Magnetite Nanoparticles Using Leaf Extract of *Thymus schimperi* and their Application for Monocomponent Removal of Chromium and Mercury Ions from Aqueous Solution". J. Nanomater., 5798824. https://doi.org/10.1155/2022/5798824.

Giri, A.K., Jena, B., Biswal, B., Pradhan, A.K. et al. (2022) "Green synthesis and characterization of silver nanoparticles using *Eugenia roxburghii* DC. extract and activity against biofilm-producing bacteria". Sci Rep., 12(1), 8383. https://doi.org/10.1038/s41598-022-12484-y.

Haile Z., Mengist H.M., Dilnessa T. (2022) "Bacterial isolates, their antimicrobial susceptibility pattern, and associated factors of external ocular infections among patients attending eye clinic at Debre Markos Comprehensive Specialized Hospital, Northwest Ethiopia". PLoS One, 17(11), e0277230. https://doi.org/10.1371/journal.pone.0277230.

Hano, C. and Abbasi B.H. (2022). "Plant-Based Green Synthesis of Nanoparticles: Production, Characterization and Applications". Biomolecules, 12(1), 31. https://doi.org/10.3390/biom12010031.

Herlekar, M and Barve, S. (2015) Calcination and Microwave Assisted Biological Synthesis of Iron Oxide Nanoparticles and Comparative Efficiency Studies for Domestic Wastewater Treatment. *Int. J. Environ. Sci*., 4, 28-36. https://api.semanticscholar.org/CorpusID:41955473.

Iqbal, J., Abbasi, B.A., Yaseen, T. et al. (2021) "Green synthesis of zinc oxide nanoparticles using Elaeagnus angustifolia L. leaf extracts and their multiple in vitro biological applications". Sci Rep 11, 20988 https://doi.org/10.1038/s41598-021-99839-z.

Ismail, S.N., Kadhim, F.J., Yousif, B.A. (2023) Iron oxide nanoparticles synthesized from mixing iron (iii) nitrate salt ($Fe_2NO_3$) with (curcumin) herbs extract for antibacterial activity. *J. Surv. Fish.*, 10(3S), 1455-1464. https://doi.org/10.17762/sfs.v10i3S.583.

Kannan, S.K. and Sundrarajan, M. (2015) Biosynthesis of Yttrium oxide nanoparticles using *Acalypha indica* leaf extract. *Bull. Mater. Sci*., 38(4), 945-950. https://doi.org/10.1007/s12034-015-0927-7.

Kiwumulo, H.F., Muwonge, H., Ibingira C., Lubwama, M., *et al*. (2022) "Green synthesis and characterization of iron-oxide nanoparticles using *Moringa oleifera*: a potential protocol for use in low and middle income countries". *BMC Res Notes*, 15(1), 149. https://doi.org/10.1186/s13104-022-06039-7.

Lakshminarayanan, S., Shereen, M.F., Niraimathi, K.L., Brindha, P. *et al*. (2021). "One-pot green synthesis of iron oxide nanoparticles from *Bauhinia tomentosa*: Characterization and application towards synthesis of 1, 3 diolein". *Sci Rep*., 11, 8643. https://doi.org/10.1038/s41598-021-87960-y.

Lathakumari, R.H., Ravi, S., Trisal, S., Vajravelu, L.K., *et al*. (2022). "Efficacy of Green Synthesised Iron Oxide Nanoparticles against Various Uropathogens: A Cross-sectional Study". *J Clin of Diagn Res*., 16(10), DC05-DC10. https://www.doi.org/10.7860/JCDR/2022/58018/17065.

Lau, B.F., Kong, K.W., Leong, K.H., Sun, J. *et al*. (2020) "*Banana inflorescence*: Its bio-prospects as an ingredient for functional foods". *Trends Food Sci. Technol*., 97, 14-28. https://doi.org/10.1016/j.tifs.2019.12.023.

Lomelí-Rosales, D.A., Zamudio-Ojeda, A., Reyes-Maldonado, O.K., López-Reyes, M.E. *et al*. (2022) "Green Synthesis of Gold and Silver Nanoparticles Using Leaf Extract of Capsicum chinense Plant". *Molecules*. 27(5), 1692. https://doi.org/10.3390/molecules27051692.

Meng, L., Wei, Q., Yang, Z., Yang, D. *et al*. (2020). "Improved perovskite solar cell efficiency by tuning the colloidal size and free ion concentration in precursor solution using formic acid additive". *J. Energy Chem*., 41, 43-51. https://doi.org/10.1016/j.jechem.2019.04.019.

Meziane, H., Laita, M., Azzaoui, K., Boulouiz, A., Neffa, M., Sabbahi, R., Nandiyanto, A. B. D., El Idrissi, A., Abidi, N., Siaj, M., Touzani, R. (2024). Nanocellulose fibers: A Review of Preparation Methods, Characterization Techniques, and Reinforcement Applications. *Mor. J. Chem*., 12, 1, 305-343.https://doi.org/10.48317/IMIST.PRSM/morjchem-v12i1.44573

Mohamed, A., Atta, R.R., Kotp, A.A., Abo El-Ela, F.I. *et al*. (2023). "Green synthesis and characterization of iron oxide nanoparticles for the removal of heavy metals ($Cd^{2+}$ and $Ni^{2+}$) from aqueous solutions with Antimicrobial Investigation". *Sci Rep*., 13, 7227. https://doi.org/10.1038/s41598-023-31704-7.

N.S. Yarla, N.S., Padmaja, J.I., Rao, R.P., Kirani, K.R.L.S. *et al*. (2012). "In vitro dose dependent study on anti human pathogenic bacterial and free radical scavenging activities of methanolic seed coat extract of *Borassus flabellifer L*". *Asian J Pharm Clin Res*., 12(5), 83-86. https://www.researchgate.net/publication/261251056.

Naeimipour, B, Moniri, E., Vaziri Yazdi, A., Safaeijavan, R. *et al*. (2022). "Green biosynthesis of magnetic iron oxide nanoparticles using *Mentha longifolia* for imatinib mesylate delivery". *IET Nanobiotechnol*, 16(6), 225-237. https://doi.org/10.1049%2Fnbt2.12090.

Naseer, M., Aslam, U., Khalid, B., and Chen, B. (2020). "Green route to synthesize Zinc Oxide Nanoparticles using leaf extracts of *Cassia fistula* and *Melia azadarach* and their antibacterial potential". *Sci Rep*., 10, 9055. https://doi.org/10.1038/s41598-020-65949-3.

Patra, J.K. and Baek K.H. (2014). "Green nanobiotechnology: factors affecting synthesis and characterization techniques". *J. Nanomater*., 417305. https://doi.org/10.1155/2014/417305.

Pongsuwan, C., Boonsuk, P., Sermwittayawong, D., Aiemcharoen, P. *et al*. (2022). "*Banana inflorescence waste fiber: An effective filler for starch-based bioplastics*". *Ind. Crops Prod*., 180. https://doi.org/10.1016/j.indcrop.2022.114731.

S.A. Razack, A. Suresh, S. Sriram, G. Ramakrishnan, *et al*. (2020). "Green synthesis of iron oxide nanoparticles using Hibiscus rosa-sinensis for fortifying wheat biscuits". *SN Appl. Sci*., 2, 898. https://doi.org/10.1007/s42452-020-2477-x.

Sandhya, J. and Kalaiselvam, S. (2020). "Biogenic synthesis of magnetic iron oxide nanoparticles using inedible Borassus flabellifer seed coat: characterization, antimicrobial, antioxidant activity and in vitro cytotoxicity analysis". *Mater. Res. Express*., 7, 015045. https://doi.org/10.1088/2053-1591/ab6642.

Shabbir, M.A., Naveed, M., ur Rehman, S., ul Ain, N., *et al*. (2023). "Synthesis of Iron Oxide Nanoparticles f66rom Madhuca indica Plant Extract and Assessment of Their Cytotoxic, Antioxidant, Anti-Inflammatory, and Anti-Diabetic Properties via Different Nanoinformatics Approaches". *ACS Omega*, 8(37), 33358-33366. https://doi.org/10.1021/acsomega.3c02744.

Singh, K., Chopra, D.S., Singh, S. and Singh, N. (2020) "Optimization and ecofriendly synthesis of iron oxide nanoparticles as potential antioxidant". *Arab. J. Chem*., 13, 9034-9046. https://doi.org/10.1016/j.arabjc.2020.10.025.

Sivakami, M., Devi, K.R., Renuka, R. and Thilagavathi, T. (2020). "Green synthesis of magnetic nanoparticles via *Cinnamomum verum* bark extract for biological application". *J. Environ. Chem. Eng*., 8, 04420. https://doi.org/10.1016/j.jece.2020.104420.

Skłodowski, K., Chmielewska-Deptuła, S.J., Piktel, E., Wolak, P. *et al*. (2023). "Metallic Nanosystems in the Development of Antimicrobial Strategies with High Antimicrobial Activity and High Biocompatibility". *Int J Mol Sci*., 24(3), 2104. https://doi.org/10.3390/ijms24032104.

Sulthana, M.R. and Madhavan, M.S. (2022) "Green synthesis, characterization, and antibacterial activity of iron oxide nanoparticles derived from *Solanum nigrum* leaf extract". *Int. J. Adv. Res. Biol. Sci*., 9(8), 131-139. http://dx.doi.org/10.22192/ijarbs.2022.09.08.013.

Tabaght, F.E., Azzaoui, K., Elidrissi, A., Hamed, O., Mejdoubi, E., Jodeh, S., Akartasse, N., Lakrat, M., Lamhamdi, A. (2021). New nanostructure based on hydroxyapatite modified cellulose for bone substitute, synthesis, and characterization. International Journal of Polymeric Materials and Polymeric Biomaterials. 70(6), 437 – 448. https://doi.org/10.1080/00914037.2020.1725758

Tabassum, N., Singh, V., Chaturvedi, V.K. and Vamanu, E. (2023) "A facile synthesis of flower-like iron oxide nanoparticles and its efficacy measurements for antibacterial, cytotoxicity and antioxidant activity". *Pharmaceutics*, 15(6), 1726. https://doi.org/10.3390/pharmaceutics15061726.

Thenmozhi, T., Rasajna, N., Rajesh, M. and Sushma, N.J. (2019). "Biosynthesis and Characterization of Iron Oxide Nanoparticles via Syzygium aromaticum Extract and Determination of Its Cytotoxicity against Human Breast Cancer Cell Lines". *J. Nanosci. Tech*., 5(1), 587-592. https://doi.org/10.30799/jnst.178.19050103.

Villaño D., Fernández-Pachón M.S., Moyá M.L., Troncoso A.M. *et al*. (2007). "Radical scavenging ability of polyphenolic compounds towards DPPH free radical". *Talanta*, 71(1), 230-235. https://doi.org/10.1016/j.talanta.2006.03.050.

Yahyaoui R., Azzaoui K., Lamhamdi A., Mejdoubi E., Elabed S., Hammouti B. (2014). Preparation of oxygenated apatite from hydrolysis of cured brushite cement in aqueous medium. *Der Pharma Chemica.* 6(6), 133 – 138. ISSN 0975413X

(2024); http://www.jmaterenvironsci.com